resulting power transmissivity $\overline{H}_1 \cdot \overline{H}_1^* = \bar{\tau}(x)/\tau_0$. A small unevenness is seen to reduce the transmissivity only in the center part of the transmission band ($b = 0.5$). A larger unevenness also affects its wings, they are slightly increased.

The peak transmission τ_0 of the ideal FPI is reduced by the unevenness to $\bar{\tau}_0$, and the bandwidth, measured between the points 0.5 $\bar{\tau}_0$, is increased from $2\pi/F$ to $2\pi/\overline{F}$ in the x scale. In Fig. 14 the ratios $\bar{\tau}_0/\tau_0$ and $\overline{F}/F$ are plotted vs b, the parameter of unevenness. The properties of the FPI remain essentially unchanged by an unevenness up to $b = 0.1$, that is up to $\Delta d \leq 0.1\lambda/(4nF)$. An unevenness of the order $\Delta d \simeq \lambda/(4nF)$ reduces, however, both F and τ_0 to approximately half their ideal values. It is remarkable that for a given unevenness F and τ_0 are reduced by nearly the same factor,

$$\overline{F}/F \simeq \bar{\tau}_0/\tau_0. \tag{22}$$

This fact is not determined by the special assumption (19) for the distribution of spacings. It results for all reasonable distributions if they are not too broad. The amplitude transmissivity is obtained by weighting $H_1(x)$ (see curve $b = 0$ in Fig. 12) with the distribution function. If the distribution is narrow, this averaging process reduces the center part of the transmission band and has negligible influence on the wings, as it was already observed for the special distribution (19). As a consequence the points $x_{1/2}$ of half-maximum intensity are shifted approximately along the power transmission curve of the ideal FPI which is the curve $b = 0$ in Fig. 13.

$$\tau(x)/\tau_0 \simeq H_1(x)H_1^*(x) = (1 + x^2)^{-1}. \tag{23}$$

The shift goes from $x_{1/2} = \pm 1$ to $\bar{x}_{1/2} = \pm(2\bar{\tau}_0/\tau_0 - 1)^{1/2}$ and results in a decrease of the finesse.

$$\frac{\overline{F}}{F} = \frac{x_{1/2}}{\bar{x}_{1/2}} = \frac{\bar{\tau}_0}{\tau_0} \cdot \left(2\frac{\bar{\tau}_0}{\tau_0} - \frac{\bar{\tau}_0^2}{\tau_0^2}\right)^{-1/2}. \tag{24}$$

The value of the last bracket is only slightly different from 1. It lies between 0.9 and 1 for $0.6 \leq \bar{\tau}_0/\tau_0 \leq 1$. Therefore, in good approximation (22) should hold for all reasonable distributions of spacing as long as this ratio (22) is ≥ 0.6.

A relation of the type (22) is observed between the experimental and theoretical values in Figs. 8 and 9. Using Fig. 14 the magnitude of the unevenness and of the error in parallelism is estimated to be $\Delta d = 1.5 \cdots 2\ \mu$ for both types of FPI's.

ACKNOWLEDGMENT

The authors are indebted to the editors for their comments and suggestions. They also wish to thank the Deutsche Forschungsgemeinschaft which has supported the construction of the grating spectrometer.

Spherical Mirror Fabry-Perot Resonators*

ROBERT W. ZIMMERER†, SENIOR MEMBER, IEEE

Summary—**An experimental investigation of the Fabry-Perot Interfometer (FPS) using spherical mirrors is reported. The FPS was operated as a microwave resonant cavity at 60 to 70 Gc. Measurements were made of the loss and coupling as a function of mirror spacing. The electric field variation within the resonator was also measured. Other characteristics of the spherical Fabry-Perot resonator were observed and are discussed.**

A qualitative discussion of the behavior of a spheroidal cavity resonator is presented and its relation to the FPS and beam waveguide is demonstrated.

INTRODUCTION

THE SPHERICAL mirror Fabry-Perot Interferomter (FPS) was first introduced as a new optical instrument by Connes [1]. In a series of papers [1], [2], he developed a geometrical optics theory and application of the instrument. With the advent of the laser the FPS was employed as a resonator and an electromagnetic theory of its operation was developed by several investigators at Bell Telephone Laboratories [3]–[7]. In a parallel development of the beam waveguide for the transmission of quasi-optical microwave power, Goubau and his associates have developed an electromagnetic theory [8] which has many applications to the FPS. The application and experimental verification of these various theories has been most rapid. The direct observation of laser output [9], the successful operation of the microwave FPS [10], [11], the transmission line studies of the beam waveguide [12]–[15], all verified the theoretical soundness of the work.

We have constructed and operated a variety of microwave Fabry-Perot resonators of both planar and spheri-

* Received April 29, 1963; revised manuscript received June 20, 1963. A preliminary note on this work has been published by the author, "Experimental investigation of Fabry-Perot interferometers," PROC. IRE (*Correspondence*), vol. 51, pp. 475–476; March, 1963.

† National Bureau of Standards, Boulder, Colo.

cal type [16]. Experimental investigation of the FPS at microwave frequencies is particularly attractive because of the comparative ease with which direct measurements of phase and amplitude can be made. We have made our measurement at wavelengths between 8 and 4 mm where klystron generators of good stability and power output are conveniently available. At these wavelengths not all the restrictions of the optical theory are satisfied while the theory of the beam waveguide is not yet extensive enough to include all aspects of the microwave FPS.

Evolution of the FPS from a Spheroidal Resonator

In our work with the FPS we have found it quite instructive to consider it as being evolved from a microwave cavity formed by rotating an ellipse about its minor axis. Such a closed surface with rotational symmetry is a special form of ellipsoid called an oblate spheroid [17]. This surface can be described by the set of equations

$$z = \frac{b}{2}\xi\cos\theta$$

$$r = \sqrt{x^2+y^2} = \frac{b}{2}\sqrt{1+\xi^2}\sin\theta \tag{1}$$

where z is measured along the axis of rotation and r perpendicular to it.

For a given b there is an oblate spheroid for every value of ξ between 0 and ∞ and a hyperboloid for each value of θ between 0 and $\pi/2$. These confocal oblate spheroids and hyerboloids constitute an orthogonal coordinate system in which Maxwell's equations can be expressed. If the wave equation is expressed in this coordinate system and the eigenfunctions are examined, a most remarkable behavior is found [18], [19]. The eigenfunctions are significantly different from zero only in the neighborhood of $\theta\sim 0$. The θ for which each eigenfunction decreases to a certain fraction of its maximum value, increases with the order of the eigenfunction and with the ratio λ/b. Thus for an oblate spheroidal resonator $b\gg\lambda$, the portion of the cavity walls far off the axis of symmetry play no appreciable role in the boundary condition that the field should vanish at the oblate spheroidal surface. Only an area on the z axis ($\theta=0$) is pertinent to this boundary condition. If the remainder of the spheroidal surface is discarded, what is left is a pair of approximately spherical mirrors. By virtue of the orthogonal coordinate system of ξ and θ, we know that the spheroidal surfaces within the resonator are surfaces of constant phase and the hyperboloids are surfaces of constant amplitude. If $b\gg\lambda$, the solution is nonzero only for θ near zero and the surfaces of constant phase are paraboloids. An examination of (1) shows that if $b\to 0$ in such a way that $b\xi/2\to\rho$ a spherical coordinate system results.

In the general case of a spheroidal cavity it is necessary to know the curvature of the approximately spherical portion on the z axis. This can be calculated from the generating ellipse. The radius of curvature of an ellipse on the minor axis is given by the square of the major axis divided by the minor axis. From (1) it follows that the radius of curvature b' of the spheroidal surface at $\theta=0$ is

$$b' = \left|\frac{1+\xi^2}{\xi}\right|\frac{b}{2}, \tag{2}$$

which can be recognized as (23) of Boyd and Gordon [5]. The relationship of the oblate spheroidal resonator to the FPS now becomes clear. The family of oblate spheroids belonging to a pair of foci of separation b generates all the possible combinations of spherical mirrors of radius of curvature b_1 and b_2 spaced a distance d. This is illustrated in Fig. 1.

$$d_1 = b_1 \pm \sqrt{b_1^2 - b^2}$$

$$d_2 = b_2 \pm \sqrt{b_2^2 - b^2}. \tag{3}$$

In the actual operation of the FPS the parameter b is not as useful as the spacing d of the mirrors.

Eliminating b from (3) we have

$$\frac{d_1}{2} = \frac{d(b_2-d)}{b_1+b_2-2d}$$

$$\frac{d_2}{2} = \frac{d(b_1-d)}{b_1+b_2-2d} \tag{4}$$

where $d_1+d_2=2d$. In this discussion it is also useful to express b in terms of the physical parameters of the FPS,

$$\frac{b}{2} = \frac{\sqrt{d(b_1-d)(b_2-d)(b_1+b_2-d)}}{b_1+b_2-2d}. \tag{5}$$

In this discussion the convention that $b_1<b_2$ is employed. As developed in part VI of Boyd and Kogelnik [6], all combinations of radii of curvature and mirror spacing are not resonant structures. From (5) it can be seen that the interfocal distance of the prototype spheroidal resonator becomes zero at four different values of the mirror spacing d. The limit $b=0$ results in a spherical coordinate system which has the familiar Bessel functions for eigenfunctions. For $b_1<d<b_2$ and $b_1+b_2<d$, b is imaginary. These are the high loss regions.

The upper diagram in Fig. 1 shows the general case for nonidentical mirrors. Note that convex mirrors, as well as concave, are allowed. The emphasized ellipse has the minimum radius of curvature on the axis and determines the special case of confocal identical mirrors symmetrically spaced about the origin. The unique degeneracy of the confocal placement of identical mirrors can be seen by noting that, from (3), any oblate spheroid with $b<b'$ will generate the required confocal mirror surfaces. In the limit $b\rightarrow 0$ the spheroid becomes a sphere with its center at one mirror or the other. This limiting case for nonidentical mirrors is illustrated in Fig. 1(b).

The general eigenfunctions for the oblate spheroidal resonator and in particular their asymptotic form for $b\gg\lambda$ are discussed in much detail by Flammer [18]. If $b\gg\lambda$ the angular functions can be expressed in terms of the Laguerre polynomials. In the limit $b/\lambda\rightarrow\infty$ the expansion contains only the first term. This is the solution obtaining for paraboloidal coordinates as developed by Pinney [20]. In the optical limit with $b/\lambda\sim 10^7$ the spherical mirror is indistinguishable from a paraboloidal mirror; in the microwave region with $b/\lambda\sim 10^2$ there is a measurable difference between these two mirrors.

In the experiment described by Christian and Goubau [12] at 24 Gc, lenses corresponding to parabolic mirrors were used and the electric field variation across the aperture was observed to be a smoothly changing function with a single maximum on the axis of the beam waveguide. In measurements of the field variation within a confocal parabolical resonator at 9.3 Gc, Beyer [14] reports very good agreement within the eigenfunction of the dominant lowest-order mode of the beam waveguide. The electric field variation measured perpendicular to the axis of a FPS at several axial positions is shown in Fig. 2. In this measurement the frequency was 61 Gc and b/λ was 115. (A discussion of the experimental method used to record these measurements is deferred to later.) It is evident that at least a fourth-order symmetric field distribution is present in what is the lowest mode of this FPS. The flat mirror was a highly polished brass surface and the spherical mirror a polished quartz mirror of optical quality with an evaporated copper surface. It is interesting to note that an equivalent spherical mirror of brass did not produce nearly as sharp a field structure. In all probability this was due to the less precise surface figure of the brass mirror which tended to "blur" the distinction between sphere and paraboloid.

The complex field structure of the FPS at microwave frequencies may be a disadvantage in some applications but this is strongly compensated by the ease with which it is aligned. The spherical surface of the mirror can be defined by a point, the center of curvature. The axis of the FPS is the line containing the two centers of curvature. If this axis intersects each mirror near enough to its center so that the electromagnetic fields are confined

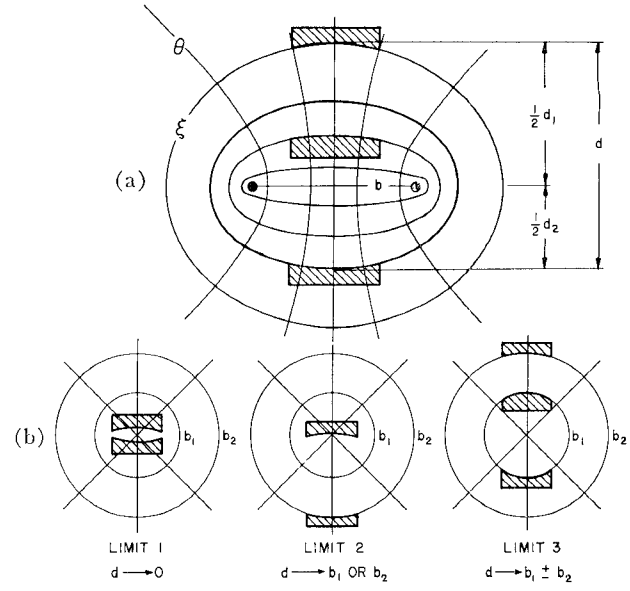

Fig. 1—Spherical mirror Fabry-Perot resonator derived from confocal oblate spheroids. (a) General case. (b) Limiting cases.

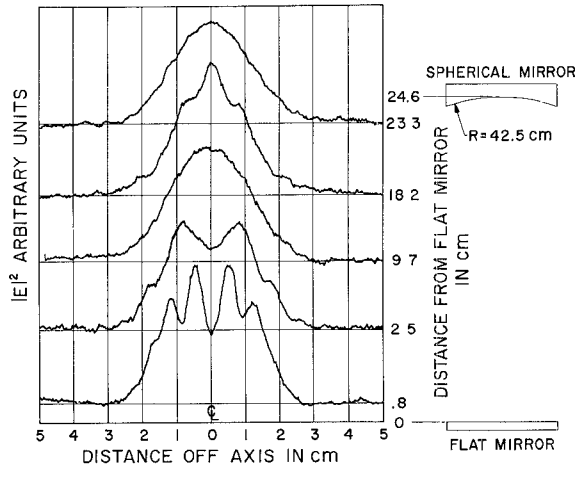

Fig. 2—Electric field variation perpendicular to resonator axis and electric field.

entirely within the mirror aperture, the FPS is aligned. A small rotation of one mirror can be corrected by an axial translation. This is not the case with either the planar Fabry-Perot or the parabolic mirror resonator. These mirror surfaces are characterized by an axis or normal. Alignment is only achieved when the axis of the paraboloids coincide or the normals to the plane mirrors are parallel. A rotation of one mirror cannot be compensated by an axial translation. Resonators using at least one plane mirror can be displaced laterally keeping their axes parallel but two paraboloids have only one relative placement for correct alignment.

In our laboratory we have experienced the difficulty of aligning flat mirrors to make a microwave planar Fabry-Perot resonator. Optical instruments were finally employed to simplify the tedious process. Beyer [14] re-

ports similar difficulty with paraboloids. In sharp contrast, the FPS alignment procedure is trivial. This problem of precise alignment is carried over to the beam waveguide where it affects the stability of a long transmission path containing many lenses.

The Analogy to the Beam Waveguide

Another aspect of the stability problem arises from the practical limitations of making mirrors or lenses identical. The FPS with different focal length mirrors is equivalent to a beam waveguide composed of a periodic sequence of lenses of alternating focal lengths. The transmission line analog was employed by Fox and Li [4] in their numerical calculation of the losses and mode structure of a variety of resonators. The converse analog was employed by Christian and Goubau [12] when they used a resonator to measure the losses of a beam waveguide. Such a transmission line analog is depicted in Fig. 3. One condition for stable operation would require that any image plane should recur periodically at the same relative position. This is illustrated by two planes, each at a distance x from two successive lenses of the same focal length. Using the thin lens equation of geometrical optics, $1/f=1/P+1/S$, and the relation between the focal length and radius of curvature of a mirror, $1/f=2/R$, the position on the optical axis of the image point is

$$x(1,2) = \frac{d(R_2-d) \pm \sqrt{-d(R_1-d)(R_2-d)(R_1+R_2-d)}}{R_1+R_2-2d} \quad (6)$$

where 1 and 2 refer to the two different lenses. It is apparent that both real and complex x are obtained depending upon the spacing of d. For the complex roots of x, where the complex conjugate of x is denoted by $\bar{x}$, $x(1,2)+\bar{x}(2,1)=d$. Referring to (4) and (5) the roots of (6) can be written

$$\begin{aligned} 2x(1,2) &= d_1 + ib \\ 2\bar{x}(2,1) &= d_2 - ib. \end{aligned} \quad (7)$$

This identification is shown symbolically in Fig. 4 where the elliptical section of a spheroidal resonator is superposed on the periodic sequence of lenses. This method could be extended to cover any reiterated sequence of lenses or mirrors of different focal lengths but it would not yield much more understanding of the phenomena. What is of great interest is the stability of such a transmission line when the lens spacing is nearly periodic and the focal lengths are randomly distributed about some design center as would occur in any practical application. To study this requires more sophisticated methods than geometrical optics. Similar stability problems have been considered by Pierce for electron beams [21] and beam waveguides [22] and occur in particle accelerators using periodically spaced magnets.

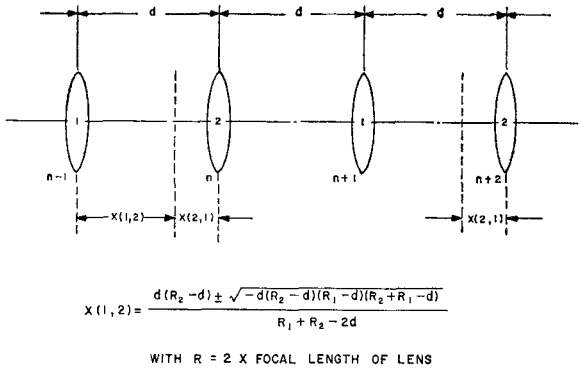

Fig. 3—Periodic sequence of simple lenses with alternating focal lengths.

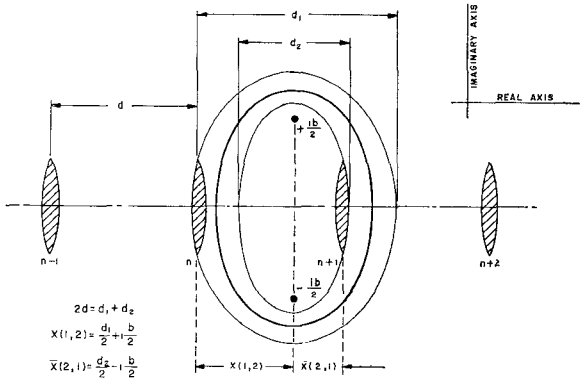

Fig. 4—Relationship of oblate spheroidal resonator to periodic sequence of lenses.

Measurement of Resonator Losses

Experimental measurements of the losses of the beam waveguide lens due to diffraction were made by Christian and Goubau [12], [13] and Beyer [14], and Beyer and Scheibe [15]. These experiments consisted of operating confocal paraboloidal resonators and measuring the Q of the resonator. We have measured the loss of the FPS as a function of mirror spacing for resonators using both identical and nonidentical mirrors. Several resonators were constructed using different combinations of spherical mirrors.

The FPS was operated as a microwave reaction cavity in order to have one mirror free to move. The fixed mirror was 12 cm in diamter with an RG-98u or RG-99u waveguide feed at the center. A coupling hole of diameter equal to the short waveguide dimension was drilled through the mirror. The iris was as thin as possible, about 0.010 inch. The brass mirrors were turned on a lathe and polished to a specular finish. They gave rather good optical images even though surface imperfections could be seen. The mirror figures were probably of the order of 0.001 inch out of a wavelength of 0.180 inch, which is comparable to the finest optical quality obtained at optical wavelengths. Several mirrors were quartz, ground and polished to optical standards and coated with 10^{-4} cm of copper by evaporation. The figure of these mirrors was good to $10^{-4}\lambda$ at microwave

frequencies. The alignment of the FPS was accomplished by autocollimation using a small flashlight. This was a simple procedure because the FPS mirrors produced a good image of the point source.

The Q of the FPS is so high, and stable klystron sources so difficult to operate, a dynamic method of measuring Q was employed. This method was only possible because of the inherent high stability of the particular klystrons used. The klystron was connected to the FPS through a 10-db 4-port directional coupler. The bolometer detector was connected to the same side of the directional coupler as the FPS and measured the power reflected back from the FPS-waveguide junction. The klystron repeller was modulated with a low-frequency sawtooth waveform which deviated the microwave frequency some 10 Mc. The bolometer output was monotored on an osciloscope. Frequency markers were generated by a second simultaneous modulation of the klystron repeller by an RF voltage of several Mc. Such RF modulation produces sidebands of known separation which are resolved by the resonator giving absorption dips on the oscilloscope. The RF modulation is used only to calibrate the sweep length and is not present during measurements of the FPS resonance width. A typical calibration was 2 cm/Mc deviation of the klystron center frequency. The FPS-resonance width varied from 0.5 Mc to several Mc. The ratio of power absorbed by the FPS to that incident on the coupling hole, $1-|\Gamma_c|^2$, was measured simultaneously with the resonance width. The use of a bolometer had the advantage that oscilloscope deflections were proportional to power. The signal-to-noise ratio was better by an order of magnitude than with a video crystal, although there was considerable variation among bolometers and crystals. A disadvantage of the bolometer is its long time constant which requires slow sweep speeds for faithful reproduction of the sharp resonance of the FPS. Some difficulty was experienced due to a background of microwave power which "leaked" into the bolometer. This leakage varied markedly with frequency and was always minimized before making measurements.

The Q of the FPS resonator, neglecting diffraction losses, is given by the well-known relation

$$Q = q\pi/(1 - |\Gamma_m|^2) \tag{8}$$

where $|\Gamma_m|^2 \sim 1$ is the power reflection coefficient of a single mirror and $q = 2d/\lambda$, the longitudinal mode number.

The mirror reflection loss is given by

$$1 - |\Gamma_m|^2 = 4r = 4\sqrt{\frac{\omega\mu}{2g}} \tag{9}$$

where r [23] is the real part of the normalized surface impedance of a metal, and ω, μ and g have their customary meaning. The calculated value of $1-|\Gamma_m|^2$ for a copper surface at 70 Gc is about 10^{-3}.

A set of measurements of $q\pi/Q$ vs d is shown in Fig. 5 for an FPS operated at 69.5 Gc. The upper curve shows the high loss region for $b_1 < d < b_2$. The lower curve was measured using one flat mirror because of the difficulty of making two brass mirrors of identical curvature. The aperture of the movable flat mirror was large enough so that diffraction losses were due entirely to the spherical mirror. The measurements were plotted against $2d$ for ease of comparison. An attempt was made to fit a theoretical curve to the results. It was impossible to get a good fit with the upper curve but the lower curve was closely described by assuming an effective value of $a^2/b\lambda = 1.38$ instead of the actual value of 1.64.

The corresponding measurements of $1-|\Gamma_c|^2$ are shown in Fig. 6. A surprising feature is the apparent low coupling to the FPS in the far region, $d > b_2$.

To better interpret Figs. 5 and 6 it is useful to propose an equivalent microwave circuit for the general FPS. An equivalent series resonant circuit is given in Fig. 7. The FPS may be regarded as a section of beam waveguide transmission line short-circuited at each end. The characteristic impedance of this transmission line is Z_2, the voltage attenuation constant is α, the impedance of each mirror is $(1+j)R$ ohms and the reactance of the coupling hole is jX. Elementary transmission line theory [24] shows that a low but finite impedance transforms into itself in moving q half wavelengths along a low loss transmission line. The resonant nature of the length $q\lambda/2$ of the transmission line is represented by the equivalent lumped reactance and capacitance of equal magnitude $q\pi Z_2/2$. The transmission line equivalent resistance is $\alpha d Z_2$ ohms. The coupling hole transforms the input waveguide impedance into a very low impedance X^2/Z_1. The Q of a series resonant circuit is given by the quotient of the magnitude of the inductive reactance and resistance at resonance. Assuming that $Z_1 \sim Z_2 \sim Z_0$ of free space and neglecting the small quantities jX and jR compared with $q\pi Z_2/2$, we get the expected result [23].

$$Q = \frac{q\pi}{4r + 2\alpha d + 2x^2} \tag{10}$$

where

$$r = \frac{R}{Z_0} \quad \text{and} \quad x = \frac{X}{Z_0},$$

which reduces to (8) for $\alpha = x = 0$. In these experiments the FPS was undercoupled and $2r \sim 5x^2$. The quantity $1-|\Gamma_c|^2$ can be expressed in terms of the equivalent microwave circuit as

$$1 - |\Gamma_c|^2 = \frac{4z}{(1+z)^2} \tag{11}$$

with

$$z = \frac{2r + \alpha d}{x^2}. \tag{12}$$

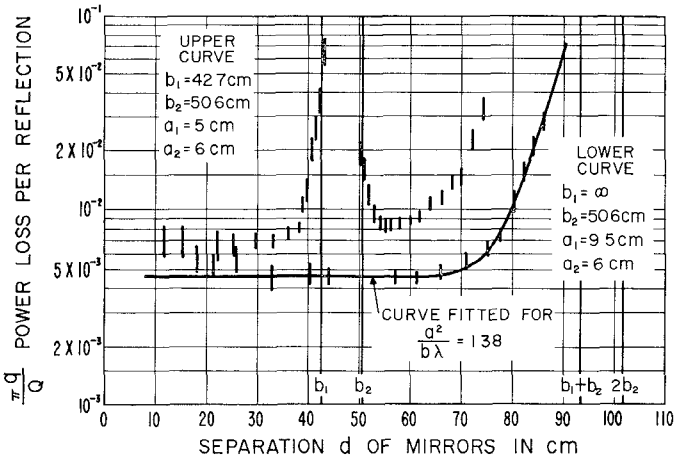

Fig. 5—Power losses in two Fabry-Perot resonators.

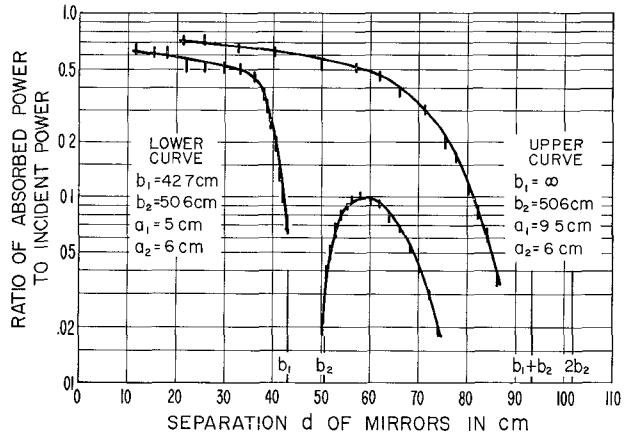

Fig. 6—Power coupling into spherical Fabry-Perot resonators.

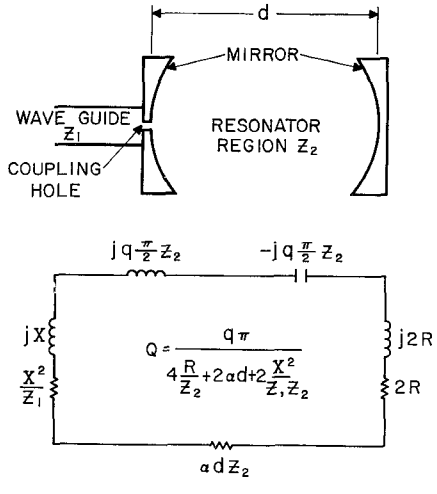

Fig. 7—Equivalent series resonant circuit of Fabry-Perot resonator.

The term αd is entirely due to absorption in the gas contained between the mirrors. At 70 Gc the normal atmospheric loss is about 0.5 db/km ($\alpha \sim 10^{-7}$ cm^{-1}) and rises as high as 15 db/km in the middle of the O_2 absorption band at 60 Gc [25]. In these measurements αd was too small to be resolved as an independent contribution to the resonator loss. The diffraction loss, α_D in the notation of Boyd and Gordon [5], was measured. Rewriting (10) in this notation,

$$Q = \frac{\pi q}{\alpha_R + \alpha_D + 2x^2} \tag{13}$$

and α_R is identified as $4r$. Rewriting (11) we get for large values of $\alpha_D + \alpha_R$,

$$1 - |\Gamma_c|^2 = \frac{(8x^2)}{\alpha_R + \alpha_D} \tag{14}$$

which is the same form as the expression for $Q/\pi q$. Since the measured value of both $1-|\Gamma_c|^2$ and $Q/\pi q$ are plotted on semilog paper, the curves should be quite similar in regions of high loss or low coupling. By superposing Figs. 5 and 6 it can be observed that this indeed is the case.

In fitting a theoretical curve to the data the expression for α_D, suggested by Boyd and Gordon [5], was used. This is

$$\alpha_D = A10^{-BN}. \tag{15}$$

They give the values of $A=10.9$ and $B=4.94$ for the TEM_{q00} mode with the square mirror. It was found that better argeement was obtained using the values $A=29$ and $B=4.83$ which fit the curve of α_D as given by Beyer and Scheibe [15] and Fox and Li [4] for the TEM_{q00} mode with a circular mirror. From (43) of Boyd and Kogelnik we obtain

$$N_1 = \frac{a_1^2}{b_1\lambda}\left[\frac{2}{s_1} - 1\right]^{1/2}$$

$$N_2 = \frac{a_2^2}{b_2\lambda}\left[\frac{2}{s_2} - 1\right]^{1/2}, \tag{16}$$

with $s_1 = d_1/b_1$, $s_2 = d_2/b_2$, and d_1 and d_2 defined by (3) and (4). Because only one mirror contributed to the diffraction loss in the FPS when using one flat and one spherical mirror, (13) was modified to give

$$\frac{\pi q}{Q} = \alpha_R + \tfrac{1}{2}\alpha_D + 2x^2 \tag{17}$$

as the equation of the curve with α_D determined from (15) and (16). The measured value 4.6×10^{-3} was used for the quantity $\alpha_R + 2x^2$. This compares with $\alpha_R = 10^{-3}$ computed for copper by (9).

It is expected that an extremum should be observed in the far region for both $q\pi/Q$ and $1-|\Gamma_c|^2$ for $b_1 \neq b_2$. From (3) and (16) it can be seen that this should occur when $b=b_1$, whereupon $2d=b_1+b_2+\sqrt{(b_2^2-b_1^2)}$. For these measurements the extremum should occur at $d=60.3$ cm. This agrees well with the $1-|\Gamma_c|^2$ data but not with the $q\pi/Q$ measurements.

An interesting feature of these data is that the coupling to the FPS is lower in the far region, $d>b_2$ than in the near region $d<b_1$ by an order of magnitude. If the FPS axis moved away from the coupling hole in going from $d=40$ to $d=60$ cm, the field of the resonator at the coupling hole could be smaller than the maximum and account for the decreased coupling. Attempts to realign the FPS have shown this not be to the explanation. This effect is real and occurs in all the FPS of this type we have operated. In view of the complex field structure with in the FPS, a possible explanation is a relative decrease of field strength on the axis compared to the average field across the aperture as d increases. This would account for the gradual decrease in coupling shown in the upper curve of Fig. 6 as d goes from 0 to 60 cm.

Measurement of Field Distribution

At this point it is appropriate to mention that the field of the FPS was measured by moving a small lossy paper disk across the mirror aperture and recording the change in power absorbed by the cavity $(1-|\Gamma_c|^2)$. If the object is of small volume compared with the active resonator volume, low loss compared with the natural resonator losses, and dielectric and magnetic properties nearly that of free space, it will have very little perturbing effect on the field and can be represented as an added series resistance in the equivalent circuit. The equivalent resistance will be very nearly proportional to the square of the local electric field. The reflected resistance z of the FPS at resonance normalized to the waveguide impedance varied from about 6 to 9 in these field measurements as the probe moved from zero to maximum field locations. From (11) it can be found that $1-|\Gamma_c|^2$ is linear to 4 per cent for this change in z.

The paper disk was supported by a nylon thread passing through its center and wound on the shaft of a 0.1-per cent helipot. As the helipot shaft was rotated the paper disk moved across the mirror aperture at right angles to the plane of the electric field. A voltage developed by the helipot referenced its lateral position. The paper disk was about 2λ in diameter. To use an unstabilized klystron with a FPS of $Q\sim10^5$, the klystron was swept in frequency as previously described. The peak of the bolometer output corresponded to $1-|\Gamma_c|^2$ at resonance. Detuning effects and sweep to sweep frequency changes were greatly minimized by using a peak detector to rectify the ac signal from the bolometer. Thus two dc voltages were derived to operate an XY recorder which made the traces of Fig. 2. The complex field pattern of Fig. 2 is strongly dependent on the mirror spacing. This phenomenon appears to be real and not caused by the presence of the probe within the resonator. Further study of this is being undertaken.

Resonance Within the High Loss Region

The experiments indicate that the resonances persist into the high loss region where the present FPS theory is not valid [26]. It is of interest to estimate how close to the high loss regions the approximate theory should be valid. To do this we might say that b, the interfocal distance of the spheroidal prototype resonator, should be at least 20λ. If we let d approach to within ϵ, the 4 limiting mirror separations, we obtain for ϵ the following minimum values:

$$\epsilon = 100\lambda^2\left(\frac{1}{b_1}-\frac{1}{b_2}\right) \qquad \begin{matrix} d\to b_1-\epsilon \\ d\to b_2+\epsilon \end{matrix} \tag{18}$$

$$= 100^2\left(\frac{1}{b_1}+\frac{1}{b_2}\right) \qquad \begin{matrix} d\to \epsilon \\ d\to b_1+b_2-\epsilon. \end{matrix} \tag{19}$$

For this FPS $\epsilon=0.16$ cm, $\epsilon=2.0$ cm, a rather close approach to the boundaries of the high loss region.

Our work demonstrates that within the central high loss region there are two TEM_{q00} resonances present which can be identified as belonging to the two low loss regions. They occur at slightly different values of the mirror spacing d. The one is decaying as the other is growing with increasing d. It seems reasonable to define a wavelength within the resonator to be twice the distance the mirrors must be displaced to change q by unity. From (47) of Boyd and Kogelnik we have

$$\frac{q}{2}=\frac{d}{\lambda}-\frac{1+m+n}{2\pi}\cos^{-1}(1-s) \tag{20}$$

where $s=d/b'$. Calculating $\Delta q/2\Delta d$ we get the Taylor Series expansion.

$$\frac{\Delta q}{2\Delta d}=\frac{1}{\lambda_g}=\frac{1}{\lambda}-\frac{1+m+n}{2\pi b'\sqrt{s(2-s)}} \cdot\left\{1-\frac{1-s}{s(2-s)}\frac{\lambda_g}{4b'} + \frac{2s^2-4s+3}{s^2(2-s)^2}\frac{\lambda_g^2}{24b'^2}+\cdots\right\} \tag{21}$$

where Δd has been put equal to $\lambda_g/2$. Near the confocal spacing, $s\sim1$ and (21) simplifies to

$$\lambda_g=\lambda\left[1-\frac{1+m+n}{2\pi}\frac{\lambda}{b'}\right]^{-1}. \tag{22}$$

If λ_g is computed for two different FPS resonators each with identical mirrors of radius of curvature b_1 and b_2 spaced approximately confocally, we obtain a fractional difference in wavelength given by

$$\frac{\Delta\lambda_g}{\lambda} = \frac{\lambda}{2\pi}\left(\frac{1}{b_1} - \frac{1}{b_2}\right) \tag{23}$$

where $q = (2d/\lambda) \gg 1$ and λ is very nearly equal to λ_g. Assuming that the two nearly coincident TEM_{qoo} resonances within the high loss region belong to the same q, but to slightly different values of λ_g, one can compute the fractional difference in wavelength from (23) to be

$$\Delta d = q\frac{\Delta\lambda_g}{2}$$

or

$$\frac{\Delta\lambda_g}{\lambda} = \frac{\Delta d}{d}. \tag{24}$$

Measurements on several FPS gave excellent agreement with this interpretation. Δd was of the order 0.004 inch, just about the limit for reading the micrometer mirror adjustment. The assignment of wavelengths to the two low loss regions was in agreement with (22), the near region $d < b_1$ having the longer λ_g and the far region $d > b_2$ having the shorter λ_g.

The definition of λ_g as given by (22) has been verified to within the error of experimental measurements of λ_g by simultaneous measurement of the frequency to some six places. For the larger FPS the free-space wavelength λ agreed with the resonator wavelength λ_g to the 3 figure precision of the λ_g measurement. The FPS has been used with confidence in these measurements to determine the operating wavelength of the klystron. It is surprising that (22) appears to hold even for the small wavemeter constructed for RG-98/u waveguide [26]. In that instrument the radius of curvature of the mirrors is only 10λ and since it is operated confocally b of (5) is also 10λ.

Higher-Order Modes

Qualitative verification was made of the existence of higher-order TEM_{dmn} modes. These were quite conspicuous at close mirror spacing and in fact could be easily confused with the dominant TEM_{qoo} mode because of their prominence. At no time could clear evidence be found of the axially symmetric "bulls eye" modes. These are predicted for circular mirrors from beam waveguide theory [8] as well as being one of the results obtained by Fox and Li [4] (Boyd and Kogelnik [6] compare these formulations in the appendix to their paper). The mirrors could always be readjusted to resolve a single resonance peak of a higher-order mode into two or more individual resonances. These multiplets could be shown to have different numbers of maxima along the electric field and at right angles to it. In this respect they conformed to the square mirror theory of Boyd and Gordon, with the degeneracy in m and n removed by a small difference in the radius of curvature in the x-z and y-z planes.

The true surface of a real mirror can be considered to have one or more zones where the curvature is constant and each zone would form its own FPS. If the wavelength is such that the field overlaps many zones, multiplets might well occur of the type observed in these experiments. As an approximation one could replace the oblate spheroid prototype FPS by an ellipsoid with all three axes different. The FPS mirror would have two principal curvatures along orthogonal diameters. This would resemble the prototype strip mirrors of Boyd and Gordon where the square mirrors are resolved into two strip mirrors along orthogonal directions. The strip mirror in turn can be considered to be generated by an elliptical cylinder. The solution of the resonator or waveguide problem for an elliptical cylinder with interfocal distance large compared to the wavelengths gives the eigenfunctions of the FPS [19].

Many variations of the FPS have already been considered by those working with them such as using two cylindrical reflectors at right angles (circular, elliptical, or parabolic), or unfolding the resonator to make a beam waveguide using mirrors instead of lenses. Undoubtedly many more applications of the FPS will be invented as microwave technology makes increasing use of physical optics.

References

[1] P. Connes, "Enhancement of the product of luminosity by resolution of an interferometer using a path difference independent of incidence," *Rev. Opt.*, vol. 35, pp. 37–43; January, 1956.

[2] ——, "The spherical Fabry-Perot etalon," *J. Phys. Rad.*, vol. 19, pp. 261–269; March, 1958.

[3] Since this work was presented at the Orlando Conference, a further paper by A. G. Fox and T. Li, "Modes in a maser interferometer with curved and tilted mirrors," Proc. IEEE, vol. 51, pp. 80–89; January, 1963, has appeared which discusses the nature of the resonances within the high loss region. These are not allowed in the approximate theory of Boyd and Kogelnik.

[4] A. G. Fox and T. Li, "Resonant modes in a maser interferometer," *Bell Sys. Tech. J.*, vol. 40, pp. 453–488; March, 1961.

[5] G. Boyd and J. Gordon, "Confocal multimode resonator for millimeter through optical wavelength masers," *Bell. Sys. Tech. J.*, vol. 40, pp. 489–508; March, 1961.

[6] G. Boyd and H. Kogelnik, "Generalized confocal resonator theory," *Bell Sys. Tech. J.*, vol. 41, pp. 1347–1369; July, 1962.

[7] D. Kleinman and P. Kisliuk, "Discrimination against unwanted orders in the Fabry-Perot resonator," *Bell. Sys. Tech. J.*, vol. 41, pp. 453–462; March, 1962. Comments on this paper have been made by A. G. Fox, T. Li, D. Kleinman, and P. Kisliuk, *Bell. Sys. Tech. J.*, vol. 41, pp. 1475–1476; July, 1962, and successful application of the suggestion is given by H. Kogelnik and C. Patel, "Mode suppression and single frequency operation in gaseous optical masers," Proc. IRE (*Correspondence*), vol. 50, pp. 2365–2366; November, 1962.

[8] G. Goubau and F. Schwering, "On the guided propagation of electromagnetic wave beams," IRE Trans. on Antennas and Propagation, vol. AP-9, pp. 248–256; May, 1961.

[9] D. Herriott, "Optical properties of a continuous He-He maser," *J. Opt. Soc. Am.*, vol. 52, pp. 31–37; January, 1962. See also, W. W. Rigrod, "Isolation of axi-symmetrical modes," *Appl. Phys. Letters*, vol. 2, p. 51; February, 1963.

[10] D. Marcuse, "HCN molecular beam-type maser," IRE Trans. on Instrumentation, vol. I 11, pp. 187–190; December, 1962.

[11] E. H. Scheibe, "Measurements on resonators formed from circular plane and confocal paraboloidal mirrors," Proc. IRE (*Correspondence*), vol. 49, p. 1079; June, 1961.

[12] J. Christian and G. Goubau, "Experimental studies on a beam waveguide for millimeter waves," IRE TRANS. ON ANTENNAS AND PROPAGATION, vol. AP-9, pp. 256–263; May, 1961.
[13] J. Christian and G. Goubau, "Some measurements on an iris beam waveguide," PROC. IRE (*Correspondence*), vol. 49, pp. 1679–1680; November, 1961.
[14] J. Beyer, "Study of the Beam Waveguide," Ph.D. thesis, University of Wisconsin, Madison, 1961; University Microfilms, Inc., Ann Arbor, Mich. A portion of this work has been published: J. Beyer and E. Scheibe, "Loss measurements of the beam waveguide," IEEE TRANS. on MICROWAVE THEORY AND TECHNIQUES, vol. MTT-11, pp. 18–22; January, 1963.
[15] J. Beyer and E. Scheibe, "Higher modes in guided electromagnetic wave beams," IRE TRANS. ON ANTENNAS AND PROPAGATION (*Correspondence*), vol. AP-10, pp. 349–350; May, 1962.
[16] Y. Beers, R. Zimmerer, G. Strine, and M. V. Anderson, "Millimeter wavelength resonant structures," IEEE TRANS. ON MICROWAVE THEORY AND TECHNIQUES, vol. MIT-11, pp. 142–149; March, 1963. See also, W. Culshaw, "Resonator for millimeter and submillimeter wavelengths," IEEE TRANS. ON MICROWAVE THEORY AND TECHNIQUES, vol. MTT-9, pp. 135–144; March, 1961.
[17] The use of ellipsoidal microwave cavities has not been extensive. This is in part due to the difficulty of theoretical anlaysis. Two such theoretical investigations are recorded in the literature and pertain to this discussion. The word confocal is used both in its geometrical sense as confocal ellipses and optical sense of lenses having a common focal point. J. C. Simons, "Electromagnetic Resonant Behavior of a Confocal Spheroidal Cavity System in the Microwave Region," Ph.D. thesis, M.I.T., Cambridge; 1950. H. Geppert and H. Schmid, "Confocal Ellipsoidal Shells as Electromagnetic Cavity Resonators," Wartime Rept. of the Mathematical Institute of the University of Berlin, Germany; available from ASTIA as Document ATI 32573, May, 1944.
[18] C. Flammer, "Spheroidal Wave Functions," Stanford University Press, Palo Alto, Calif., Ch. 8.2; 1957.
[19] See for example the discussion of the Scalar wave equation in elliptic cylinder coordinates for $b \gg \lambda$ in P. Morse and H. Feshbach, "Methods of Theoretical Physics," McGraw-Hill Book Co , Inc., New York, N. Y., pp. 1416–1420; 1953.
[20] E. Pinney, "Electromagnetic fields in a paraboloidal reflector," *J. Math. and Phys.*, vol. 26, pp. 42–55; 1947.
[21] J. R. Pierce, "Theory and Design of Electron Beams," D. Van Nostrand and Co., New York, N. Y.; 1954.
[22] ——, "Modes in sequences of lenses," *Nat'l. Acad. of Sci.*, vol. 47, pp. 1808–1813; November, 1961.
[23] The conventional use of r, R and z, Z and x, X in the following discussion to represent impedance and reactance should not be confused with the earlier use of the same symbols for coordinates.
[24] This particular application is discussed in C. G. Montgomery, R. H. Dicke, and E. M. Purcell, "Principles of Microwave Circuits," McGraw-Hill Book Company, Inc., New York, N. Y. sec. 7.10; 1948.
[25] E. Rosenblum, "Atmospheric absorption of 10-400 Gcs radiation," *Microwave J.*, vol. 4, pp. 91–96; March, 1961.
[26] R. Zimmerer, "New wavemeter for millimeter wavelengths," *Rev. Sci. Instr.*, vol. 33, pp. 858–859; August, 1962.

Microwave Type Bolometer for Submillimeter Wave Measurements*

J. F. BYRNE†, FELLOW, IEEE, AND C. F. COOK‡

Summary—**An approach to the problem of submillimeter wave measurement through the extension of microwave techniques has led to the development of a submillimeter bolometer with the sensitivity requisite to calibration with a thermal source. The sensor employs conventional components, horn, waveguide and coaxial line, with a novel coax-to-guide transition consisting of part of the bolometer element, the rest of which serves as a center conductor of the coaxial lines. The entire set of submillimeter components is contained in a $\frac{1}{4}$-inch block of metal. Fundamental problems of detection in this band are discussed with application to the sensor. Calibration techniques and data taken with the instrument are reported.**

INTRODUCTION

THE SENSOR described in this paper is the outcome of an effort to provide a method of measurement of radiation in the wavelength region around and below one millimeter. In approaching the problem of submillimeter wave measurement it was decided that the equipment design might well be benefited through the extension of microwave technologies into this portion of the spectrum rather than the alternate approach which would be to attack the problem from the infrared point of view.

A prime advantage of the microwave view was the likelihood that the number of unknown quantities could be minimized through the almost exclusive use of metallic elements in the system. The bolometer design finally adopted essentially consists of a horn antenna feeding a submillimeter waveguide which is terminated in a novel waveguide to coax transition section. The coaxial section has a center conductor of Wollaston wire of extremely small size and high loss per unit length. The termination of the coaxial section is of little importance because of the high loss along the coax. The waveguide is thus terminated in a transition to coax with a "lossy" line as the load.

SENSOR CONFIGURATION

Fig. 1 shows the sensor configuration. The bolometer wire serves both as the center conductors of the two lossy coaxial lines and the probe which couples the waveguide and the coax system. The probe crosses the wave-

* Received January 21, 1963. This paper was presented at the IEEE Millimeter and Submillimeter Conference, Orlando, Fla. January 7–10, 1963.
† Motorola Inc., Technical Products Divisions, Phoenix, Ariz.
‡ Motorola Inc., Systems Research Laboratory, Riverside, Calif.